RESEARCH ARTICLE

The fatty acid transport protein Fat1p is involved in the export of fatty acids from lipid bodies in *Yarrowia lipolytica*

Rémi Dulermo[1,2], Heber Gamboa-Meléndez[1,2], Thierry Dulermo[1,2], France Thevenieau[3] & Jean-Marc Nicaud[1,2]

[1]UMR1319 Micalis, INRA, Jouy-en-Josas, France; [2]UMR Micalis, AgroParisTech, Jouy-en-Josas, France; and [3]Direction Innovation, SOFIPROTEOL, Paris, France

Correspondence: Jean-Marc Nicaud, Institut Micalis, UMR1319, Team BIMLip: Biologie Intégrative du Métabolisme Lipidique, CBAI, INRA-AgroParisTech, F-78850 Thiverval-Grignon, France. Tel.: +33 130815450; fax: +33 130815457; e-mail: jean-marc.nicaud@grignon.inra.fr

Received 12 May 2014; revised 9 June 2014; accepted 12 June 2014. Final version published online 08 July 2014.

DOI: 10.1111/1567-1364.12177

Editor: Jens Nielsen

Keywords
fatty acid accumulation; fatty acid remobilisation; fatty acid transport; lipid body; peroxisome.

Abstract

In order to live, cells need to import different molecules, such as sugars, amino acids or lipids, using transporters. In *Saccharomyces cerevisiae*, the *ScFAT1* gene encodes the long-chain fatty acid transporter; however, the transport of fatty acids (FAs) in the oleaginous yeast *Yarrowia lipolytica* has not yet been studied. In contrast to what has previously been found for Δ*Scfat1* strains, Δ*Ylfat1* yeast was still able to grow on substrates containing short-, medium- or long-chain FAs. We observed a notable difference in cell lipid content between wild-type (WT) and deletion mutant strains after 24 h of culture in minimal oleate medium: in the WT strain, lipids represented 24% of cell dry weight (CDW), while they accounted for 37% of CDW in the Δ*Ylfat1* strain. This result indicates that YlFat1p is not involved in cell lipid uptake. Moreover, we also observed that fatty acid remobilisation was decreased in the Δ*Ylfat1* strain and that fluorescence-tagged YlFat1p proteins localised to the interfaces between lipid bodies, which suggests that YlFat1p may play a role in the export of FAs from lipid bodies.

Introduction

Fatty acids (FAs) serve as essential nutritional cues to cells because they are components of the plasma membrane, endoplasmic reticulum, mitochondria and peroxisome, in addition to being the building blocks of phospholipids and sterols. In yeast, the breakdown of lipids via β-oxidation takes place in peroxisomes, and this process ultimately yields significant energy for cells. Although cells have the ability to synthesise FAs, this process is more energy intensive, and therefore less favoured, than the uptake of FAs from the extracellular medium. In the latter process, acyl-CoA synthetases add a CoA group to exogenous FAs, thus activating them so that they can enter the cell (Kohlwein *et al.*, 2013).

In *Saccharomyces cerevisiae*, the FA-transport system of long-chain fatty acids (LCFAs) has been well characterised. In this yeast, the transport of LCFAs is mediated by the transporter ScFat1p and the fatty acyl-CoA synthetases ScFaa1p and ScFaa4p, which couple the transport of exogenous FAs into the cell with their activation via the addition of CoA group (Duronio *et al.*, 1992; Johnson *et al.*, 1994; Knoll *et al.*, 1994; Zou *et al.*, 2003). In yeast, fatty acid import is saturable and dependent upon ScFat1p, a homologue of the murine fatty acid transport protein (Faergeman *et al.*, 1997; Dirusso *et al.*, 2000). Indeed, whereas a wild-type (WT) strain was able to grow on YPD medium that contained cerulenin (a drug that inhibits fatty acid synthesis) in addition to oleate, myristate or palmitate, the growth of Δ*Scfat1* mutants was partially reduced on myristate or palmitate and strongly inhibited on oleate (Faergeman *et al.*, 1997). In addition, the WT strain was able to accumulate fluorescent long-chain fatty acid analogues (C_1-BODIPY-C_{12}), whereas Δ*Scfat1* was not (Faergeman *et al.*, 1997; Dirusso *et al.*, 2000). However, Δ*Scfat1* was still able to transport octanoate, a medium-chain fatty acid (MCFA), which suggests that ScFat1p transport is specific to LCFAs (Dirusso *et al.*, 2000). ScFat1p has also been described to promote the activity of very long-

chain acyl-CoA synthetases (VLACS; i.e. ≥ C20), and the deletion of *ScFAT1* increased the accumulation of free very long-chain FAs in cells (Watkins *et al.*, 1998; Choi & Martin, 1999; Dirusso *et al.*, 2000). Choi & Martin (1999) suggest that ScFat1p is involved in the maintenance of cellular very long-chain fatty acid levels, probably by facilitating β-oxidation of excess intermediate length (C20-C24) species. They also proposed that growth-defective phenotype of Δ*Scfat1* is a failure to metabolise the incorporated fatty acid rather than a defect in fatty acid transport.

ScFat1p proteins contain an ATP/AMP motif (a 100-amino acid segment that is required for ATP binding and common to members of the superfamily of adenylate-forming proteins) as well as FATP/VLACS motifs (50-amino acid residues restricted to members of the FATP family) (Zou *et al.*, 2002). It has been shown that these two motifs are situated on the interior face of the plasma membrane (Obermeyer *et al.*, 2007) and that the protein–protein interaction domain of ScFat1p is probably located on the last 110 residues of the protein (Zou *et al.*, 2003; Obermeyer *et al.*, 2007). Moreover, ScFat1p has two transmembrane domains (TMs) and probably contains two additional membrane-associated helices that likely do not traverse the membrane; instead, they may anchor the protein to the membrane (Obermeyer *et al.*, 2007). Mutagenesis of *ScFAT1* has shown that some mutations in the ATP/AMP motif (S258A), in the FATP/VLACS motif (D508A, Y519A and R523A) or in the type 1 peroxisome-targeting sequence (L669) prevent proper functioning of the protein (Zou *et al.*, 2002).

Whereas LCFA transport in *S. cerevisiae* is well understood, this is not the case in most eukaryotes and, more precisely, in the oleaginous yeast *Yarrowia lipolytica*. This yeast is able to grow on a variety of hydrophobic substrates, and lipid accumulation can account for as much as 40% of cell dry weight (CDW) (Beopoulos *et al.*, 2011). As a result, this species could prove potentially quite useful for the production of biofuels (Beopoulos *et al.*, 2009). In this study, we examined the role of the ScFat1p homologue in *Y. lipolytica*, which is designated YALI0E16016p or YlFat1p. In contrast to *S. cerevisiae ScFAT1* deletion mutants, which are unable to grow on oleate-based medium, our results reveal that Δ*Ylfat1* mutant is still able to grow on oleate. Surprisingly, the Δ*Ylfat1* strain accumulated 50% more FAs than did the WT when both types of strains were grown in a medium known to promote FA accumulation. In addition, both TAG remobilisation and oleic acid β-oxidation were reduced in the mutants, although enough oxidation occurred to allow growth. Finally, YlFat1p localisation in peroxisomes and at the interface between lipid bodies indicates that the protein could be involved in the export of FAs from lipid bodies in *Y. lipolytica*.

Materials and methods

Growth and culture conditions

The *Y. lipolytica* strains used in this study were derived from the WT *Y. lipolytica* W29 strain (ATCC20460; Table 1). The auxotrophic strain used here, PO1d (Leu$^-$ Ura$^-$), was previously described by Barth & Gaillardin (1996). The prototroph derivative WT, PO1d (Leu+ Ura+), was used as WT control strain. All the strains used in this study are listed in Table 1. The media and growth conditions for *Escherichia coli* in this study are the same as those of Sambrook *et al.* (1989), and the conditions for *Y. lipolytica* are the same as those of Barth & Gaillardin (1996). Rich medium (YPD) and minimal glucose medium (YNB) were prepared as described in Mlícková *et al.* (2004). The minimal medium (YNB) contained 0.17% (w/v) yeast nitrogen base (without amino acids and ammonium sulphate, YNBww; Difco, Paris, France), 0.5% (w/v) NH_4Cl and 50 mM phosphate buffer (pH 6.8). As necessary, this minimal medium was supplemented with uracil (0.1 g L^{-1}) and/or leucine (0.1 g L^{-1}). The $YNBD_{0.5}O_3$ medium contained 0.15% (w/v) yeast extract (Bacto-BD), 0.5% glucose and 3% oleic acid. Solid media were created via the addition of 1.6% agar. The $YNBC_0$ medium was prepared in the same way as the YNB medium except that no carbon source was added (Dulermo *et al.*, 2013). When FAs were included in liquid or solid media, a 50 : 50 emulsion of FAs/10% pluronic acid was prepared and then heated at 80 °C for 10 min before being added to the media. The following FAs were used in our study: C6:0 (Sigma-Aldrich, 99%), C10:0 (Sigma-Aldrich, 99%), C14:0 (Acros Organics, 99%), C16:0 (Sigma-Aldrich, 99%) and C18:1 (Sigma-Aldrich, 70%). $YNBD_{0.5}O_3$ and $YNBC_0$ media were used for the lipid accumulation and lipid remobilisation tests, respectively. The $YNBO_{0.1}Y_{0.05}$ medium used for growth comparison of WT and Δ*Ylfat1* on fatty acid contained 0.1% oleate and 0.05% yeast extract.

Growth in microtitre plates

Overnight precultures in YPD medium (170 r.p.m., 28 °C) were centrifuged and washed with YNB; cell suspensions were standardised to an $OD_{600\ nm}$ of 0.1. Yeast strains were grown in 96-well plates in 200 μL of minimal YNB containing 1 g L^{-1} glucose. The culture was performed five times. Cultures were maintained at 28 °C under constant agitation with a Biotek Synergy MX mic-

Table 1. Strains and plasmids

Strain or plasmid	Genotype or other relevant characteristics	Source or reference
E. coli		
DH5α	*Φ80dlacZΔm15, recA1, endA1, gyrA96, thi-1, hsdR17 (r_k−, m_k+), supE44, relA1, deoR, Δ(lacZYA-argF) U169*	Promega
Y. lipolytica		
W29	*MATA, wild type*	Barth & Gaillardin (1996)
Po1d	*MATA ura3*-302 *leu2*-270 *xpr2*-322	Barth & Gaillardin (1996)
JMY330	Po1d, Ura +	Haddouche *et al.* (2010)
JMY2900	Po1d Ura$^+$ Leu$^+$, wild-type control	R. Brunel, unpublished data
JMY3148	Po1d *Ylfat1*::*URA3*ex (Leu$^-$)	This work
JMY3240	JMY3148 + *LEU2*ex (Ura$^+$ Leu$^+$)	This work
JMY3438	JMY3148 + p*TEF-ΔNter-YlFAT1-LEU2ex* (Ura$^+$ Leu$^+$)	This work
JMY3451	JMY3148 + p*TEF-YlFAT1-LEU2ex* (Ura$^+$ Leu$^+$)	This work
JMY3792	JMY3148 + p*TEF-ΔNter-YlFAT1-RedStar2-LEU2ex* (Ura$^+$ Leu$^+$)	This work
JMY3909	JMY3792 (Ura$^+$ Leu$^-$)	This work
JMY3919	JMY3909 + p*TEF-TGL4-YFP-LEU2ex* (Ura$^+$ Leu$^+$)	This work
JMY4170	JMY3148 + p*TEF-YFP-ΔNter-YlFAT1-LEU2ex* (Ura$^+$ Leu$^+$)	This work
Plasmid		
pCR4Blunt-TOPO	Cloning vector	Invitrogen
JMP547	pUB4-CRE	Fickers *et al.* (2003)
JMP803	JMP62-p*POX2-URA3ex*	Haddouche *et al.* (2010)
JMP1392	JMP62-p*TEF-RedStar2SKL-LEU2ex*	Kabran *et al.* (2012)
JMP1552	JMP62-p*TEF-TGL4-YFP-LEU2ex*	Dulermo *et al.* (2013)
JMP1762	pCR4Blunt-TOPO-*Ylfat1*::*URA3ex*	This work
JMP1911	JMP62 p*TEF-ΔNter-YlFAT1-LEU2*ex	This work
JMP1923	JMP62 p*TEF-YlFAT1-LEU2*ex	This work
JMP2127	JMP62 p*TEF-ΔNter-YlFAT1-RedStar2-LEU2*ex	This work
JMP2380	JMP62 p*TEF-YFP-ΔNter-YlFAT1-LEU2*ex	This work

rotitre plate reader (Biotek Instruments, Colmar, France); each culture's optical density at 600 nm was measured every 20 min for 24 h.

Plasmid and yeast strain construction

A schematic of the procedures used to construct the strains used in this study is depicted in Fig. 1, and the construction process is described below.

The deletion cassette was generated by PCR amplification conducted largely in accordance with the procedure of Fickers *et al.* (2003). First, the upstream (Up) and downstream (Dn) regions of the target gene were amplified using *Y. lipolytica* W29 genomic DNA as the template and the gene-specific Up and Dn oligonucleotides as primer pairs (Table 2). Primers UpI-SceI and DnIsceI contained an extension that allowed the introduction of the I-SceI restriction site, making it possible to construct an UpDn fragment via PCR fusion.

To disrupt *YlFAT1*, the primer pairs E16016Up2Not1/E16016Up2SceI and E16016Dn5Not1/E16016Dn5IsceIIceuI were employed. The resulting UpDn fragment was ligated into pCR4Blunt-TOPO. The *URA3ex* marker from JMP802 was then introduced at the I-SceI site, which yielded the *Ylfat1::URA3ex* cassette (JMP1762). The corresponding deletion cassette was obtained by NotI digestion followed by transformation via homologous recombination in *Y. lipolytica* strain PO1d; this strain was designated JMY3148 (*Ylfat1::URA3ex,* Ura$^+$ Leu$^-$). A prototrophic derivative of JMY3148 was generated by transformation with the *LEU2ex* marker, which yielded strain JMY3240 (*Ylfat1::URA3ex,* Ura$^+$ Leu$^+$).

For the Δ*Ylfat1* complementation tests, two versions of Fat1p, annotated *YlFAT1* and Δ*Nter-YlFAT1*, were amplified using the primer pairs Start-E16016-BglII/End-E16016 and Start-E16016-CPFL-BglII/E16016End, respectively (Table 2).

To determine Fat1p localisation, two tagged versions of Fat1p, Δ*Nter-YlFAT1-RedStar2* and *YFP*-Δ*Nter-YlFAT1*, were constructed by PCR. To create the former, the Δ*Nter-YlFAT1* fragment was amplified using the primer pair Start-E16016-CPFL-BglII/E16016-DsRed-Fusion, while the *RedStar2* fragment was amplified with DsRed-E16016-Fusion/DsRed-End. These PCR fragments were then mixed and joined via PCR fusion using the primer pair Start-E16016-CPFL-BglII/DsRed-End to form Δ*Nter-YlFAT1-RedStar2* (Table 2). Likewise, to create *YFP*-Δ*Nter-YlFAT1*, the Δ*Nter-YlFAT1* fragment was amplified with the primer pair E16016FYFP/End-E16016, while the

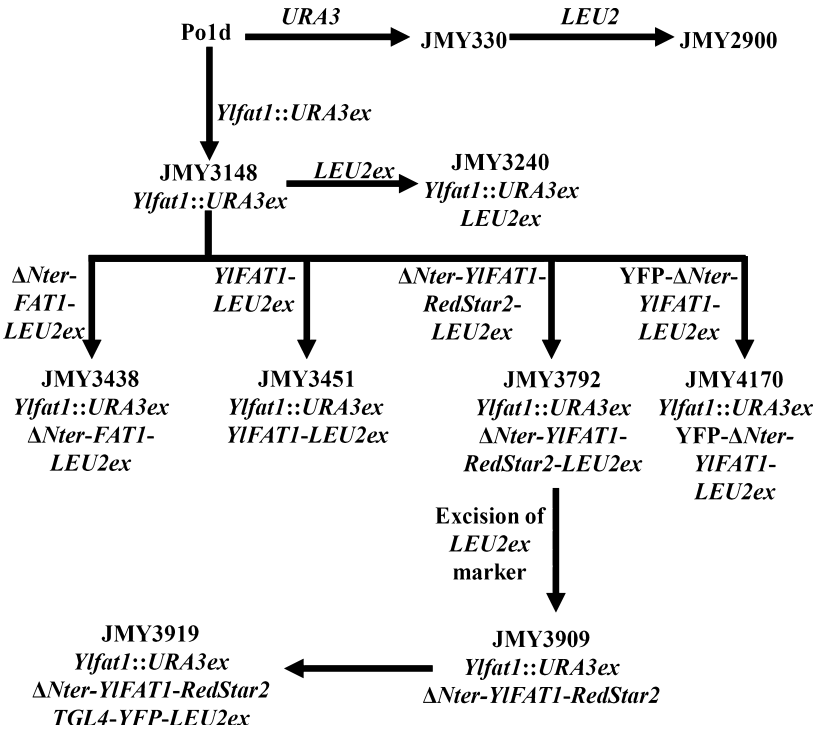

Fig. 1. Schematic representation of strain construction. The auxotrophic parental strain Po1d (Leu$^-$ Ura$^-$) was derived from WT strain W29. Transformation of the *Ylfat1::URA3ex* cassette into Po1d resulted in the creation of strain JMY3148 (*Ylfat1::URA3ex*), which carried a disrupted *YlFAT1* gene. Strain JMY3148, with *YlFAT1* deleted, was then transformed with plasmids encoding various truncated or tagged versions of YlFat1p: full length (*YlFAT1*, JMY3451); N-terminal truncated (Δ*Nter-YlFAT1*, JMY3438); RedStar2 tagged (Δ*Nter-YlFAT1-RedStar2*, JMY3792); and YFP tagged (YFP-Δ*Nter-YlFAT1*, JMY4170). Excision of the *LEU2ex* marker from JMY3792 by the plasmid JMP547 yielded JMY3909, which was subsequently transformed with a plasmid that encoded YFP-tagged TGL4 (*TGL4-YFP*, JMY3919).

Table 2. Primer list

Genes	Primers	Sequences	Utilisation
YlFAT1	E16016Up2NotI	GAATGCGGCCGCCCAATGGAACGAGTTTCAATGTCGG	Upstream fragment of *YlFAT1*
	E16016Up2SceI	CGATTACCCTGTTATCCCTACCCCTCCAAAACTGGGTATTCTGGC	
	E16016Dn5Not1	GAATGCGGCCGCTCTCGTCATTTGGCGCTTATG	Downstream fragment of *YlFAT1*
	E16016Dn5IsceIIceuI	GGTAGGGATAACAGGGTAATCGTAACTATAACGGTCCTAAGG TAGCGAGGTGATCTGGTGCGACTCAACG	
	Ver1-2E16016	CACGTAAGTAGAACAATTCAGCG	Verification of the disruption of *YlFAT1*
	Ver2-2E16016	GGTGCTGGATCTACACAGTCGAC	
	Start-E16016-BglII	ATCAGATCTCACAATGAAAACGATATTGAAAATAACAAAATCCG	Complementation/ overexpression of *Ylfat1* with *YlFAT1*
	End-E16016	CATCCTAGGTTACAGCTTAATCTTTCCGGATCC	
	Start-E16016-CPFL-BglII	ATCAGATCTCACAATGTGCCCTTTTTTAAGTCCCCTTCTCC	Complementation/ overexpression of *Ylfat1* with Δ*Nter-YlFAT1* when coupled with End-E16016
	E16016-DsRed-Fusion	GTGATGACATCTTCAGAAGAAGCACTCATCTTTCCGGATCCCAGAGAAGC	Construction of Δ*Nter-YlFAT1-RedStar2* with Start-E16016-CPFL-BglII
	DsRed-E16016-Fusion	GCTTCTCTGGGATCCGGAAAGATGAGTGCTTCTTCTGAAGATGTCATCAC	
	DsRed-End	CATCCTAGGTTACAAGAACAAGTGGTGTCTACC	
	E16016FYFP	CGGCATGGACGAGCTGTACAAGATGACAGCTGGACTAGTTGCTGCC	Construction of *YFP-ΔNter-YlFAT1*
	End-E16016	CATCCTAGGTTACAGCTTAATCTTTCCGGATCC	
	YFPBglII	ATCAGATCTCACAATGAAGCTTCCCCGCGGCCTAGGC	
	YFPFE16016	GGCAGCAACTAGTCCAGCTGTCATCTTGTACAGCTCGTCCATGCCG	
	E16016F	ATCCAGAAGATCCCCAAC	Observation of *YlFAT1* expression by RT-PCR
	E16016R	ATCGGAAGGTGTCTCCAA	
	pTEF-start	GGGTATAAAAGACCACCGTCC	Verification of expression cassette insertion into *Y. lipolytica* genome
	61stop	GTAGATAGTTGAGGTAGAAGTTG	
Actin	ACT-A1	TCCAGGCCGTCCTCTCCC	Observation of *Actin* expression by RT-PCR
	ACT-A2	GGCCAGCCATATCGAGTCGCA	
ALG9	ALG9-A1	AGTATCCCTCTGCACATGA	Observation of *ALG9* expression by RT-PCR
	ALG9-A2	TTGGCAGGAATATCGATGTC	

YFP fragment was amplified with YFPBglII/YFPFE16016. These PCR fragments were mixed and joined via PCR fusion using the primer pair YFPBglII/End-E16016 to form *YFP-ΔNter-YlFAT1* (Table 2).

To construct the expression plasmids that encoded truncated or tagged versions of YlFat1p, *YlFAT1* variants were generated by PCR; the products were then cloned into pCR4Blunt-TOPO. Sequencing was used to verify successful construction and to ensure the absence of mutations. The resulting truncated or tagged versions of Fat1p were recovered from pCR4Blunt-TOPO derivatives by BglII and AvrII digestion and ligated into BamHI- and AvrII-digested JMP1392 (Kabran *et al.*, 2012), a derivative of JMP62 plasmid (Nicaud *et al.*, 2002). The resulting plasmids (JMP1923, JMP1911, JMP2127 and JMP2380) were digested by NotI to obtain overexpression cassettes, which were subsequently transformed into JMY3148, yielding JMY3451 (Δ*Ylfat1* + p*TEF-YlFAT1*), JMY3438 (Δ*Ylfat1* + p*TEF-ΔNter-YlFAT1*), JMY3792 (Δ*Ylfat1* + p*TEF-ΔNter-YlFAT1-RedStar2*) and JMY4170 (Δ*Ylfat1* + p*TEF-YFP-ΔNter-YlFAT1*), respectively.

Disruption or overexpression cassettes were used in transformation in accordance with the lithium acetate method (Le Dall *et al.*, 1994). Transformants were selected on YNBcasa, YNBura or YNB depending on their genotype. Then, genomic DNA from yeast transformants was prepared as described by Querol *et al.* (1992). The corresponding ver1 and ver2 primers (Table 2) were used to verify gene disruption, and pTEF-start and 61 stop primers were used to verify successful insertion of the expression cassette.

Restriction enzymes were obtained from OZYME (Saint-Quentin-en-Yvelines, France). PCR amplifications were performed using an Eppendorf 2720 thermal cycler and employing GoTaq DNA polymerase (Promega) for deletion/overexpression verification and PyroBest DNA polymerase (Takara) for cloning. PCR fragments were purified using a QIAgen Purification Kit (Qiagen, Hilden, Germany), and DNA fragments were recovered from agarose gels using a QIAquick Gel Extraction Kit (Qiagen, Hilden, Germany). All the reactions were performed in accordance with the manufacturer's instructions. The CLONE MANAGER software package was used for gene sequence analysis (SCI-ED Software).

Lipid determination

Using 10–20 mg aliquots of freeze-dried cells, lipids were converted into their methyl esters using the method described in Browse *et al.* (1986). The esters produced were then used in gas chromatography (GC) analysis. The analysis was performed using a Varian 3900 gas chromatograph equipped with a flame ionisation detector and a Varian FactorFour vf-23 ms column, for which the bleed specification at 260 °C was 3 pA (30 m, 0.25 mm, 0.25 μm). FAs were quantified using the internal standard method, which involved the addition of 50 μg of commercial C17:0 (Sigma), and they were then identified by comparing their profiles to those for commercial FA methyl ester standards (FAME32; Supelco).

Analysis of *YlFAT1* expression

Precultures of the reference strain JMY2900 (WT strain) were placed in liquid YNB, supplemented with 1% glucose and 0.5% yeast extract and grown for 15 h at 28 °C. Cells were washed twice with distilled water and transferred to fresh liquid YNB media supplemented with 1% glucose, 3% oleic acid or both 1% glucose and 3% oleic acid. Cultures were incubated in baffled Erlenmeyer flasks at 28 °C and 160 r.p.m. Cultures were harvested 2 and 6 h postinoculation, frozen in liquid nitrogen and stored at −80 °C. RNA was extracted from cells using the RNeasy Mini Kit (Qiagen), and 2 μg was treated with DNase (Ambion, Life Technologies). cDNA was synthesised using the SuperScript III First-Strand RT-PCR Kit (Invitrogen). PCR was then performed using the GoTaq DNA Polymerase Kit (Promega) and employing specific primers designed by the Primer3 program (Table 2). The actin- and alpha-1,2-mannosyltransferase-encoding genes (*Actin* and *ALG9*, respectively) were used as controls.

Microscope analysis

Images were acquired using a Zeiss Axio Imager M2 microscope (Zeiss, Le Pecq, France) capable of 100× magnification and equipped with Zeiss fluorescence microscopy filters 45 and 46. AXIOVISION 4.8 software (Zeiss, Le Pecq, France) was used to acquire the images. Lipid bodies were stained by adding BodiPy® Lipid Probe (2.5 mg mL^{-1} in ethanol; Invitrogen) to the cell suspension ($A_{600\ nm}$ of 5) and letting the mixture incubate for 10 min at room temperature.

Results

Fat1p is conserved in *Y. lipolytica*

Yarrowia lipolytica is able to use different carbon sources, especially hydrophobic ones such as oil or FAs (Beopoulos *et al.*, 2011). Therefore, it is probable that its genome encodes specialised transporters for these kinds of compounds. A BLAST search for homologues of ScFat1p (YBR041W) identified YALI0E16016p (hereafter referred to as *YlFAT1*) as the only homologue in the *Y. lipolytica* genome. Curiously, its open reading frame (ORF) is

much longer than that of ScFat1p: the protein it encodes is 712 amino acids long, whereas ScFat1p is 669 amino acids long. Indeed, YlFat1p has an N-terminal extension which does not display BLAST affinity with any part of protein in the nr database, although it contains a putative mitochondrial-targeting sequence (MKTILKITKSENQ-NALFKNPISPPHPPQTRTP SLKIKVQPQIPHFFHAG-PYINRG) which was predicted by MITOPROT (http://ihg.gsf.de/ihg/mitoprot.html; Claros & Vincens, 1996) with a value of 0.98 using the first 60 amino acids of the predicted ORF. However, our results show (see section 'Lipid remobilisation is impaired in Δ*Ylfat1*') that this extension arises from a misannotation (the starting methionine was not correctly defined). We found that (1) the real YlFat1p protein is shorter (starting at the second methionine of the ORF); (2) it is composed of only 639 amino acids (Fig. 2); and (3) it shares 45% of its identity with ScFat1p. The ATP/AMP (blue frame) and FATP/VLACS (red frame) motifs are well conserved across the two proteins (Fig. 2a), suggesting that their function is also conserved. Most of the ScFat1p amino acids found to be essential by Zou *et al.* (2002), such as D508, Y519, R523 and L669R, are conserved in YlFat1p. However, YlFat1p has only one TM (TM1 $P = 0.8$; Fig. 2b), whereas ScFat1p has two (Obermeyer *et al.*, 2007; Fig. 2a; three predicted by TMHMM, Fig. 2c). Both ScFat1p and YlFat1p share the three amino acids (IKL) that are typical of a type 1 peroxisome-targeting sequence (PTS1), which addresses proteins to peroxisomes (Fig. 2a). This similarity suggests that YlFat1p may localise in peroxisomes as has been shown for ScFat1p (Natter *et al.*, 2005; van Roermund *et al.*, 2012).

YlFat1 is induced by oleate

Choi & Martin (1999) reported the surprising result that *ScFAT1* is constitutively expressed and not induced by FAs. However, as *Y. lipolytica* is able to efficiently utilise FAs, *YlFAT1* expression might be regulated by FAs. In order to test this idea, cells were grown for 15 h in YNB glucose and then transferred into fresh liquid YNB media containing glucose, oleate or both glucose and oleate. RT-PCR analyses were performed at 2 and 6 h post-transfer. We found that (1) *YlFAT1* was expressed under all the conditions tested; and (2) unlike *ScFAT1*, *YlFAT1* was upregulated in oleate-containing medium even in the presence of glucose (Fig. 3).

YlFAT1 is not essential for *Y. lipolytica* growth on FAs

ScFat1p is essential for *S. cerevisiae* growth on oleate-containing medium and is important for the species' growth on palmitate- and myristate-containing media (Faergeman *et al.*, 1997). To determine the function of *FAT1* in the oleaginous yeast *Y. lipolytica*, we inactivated *YlFAT1* in the haploid strain Po1d using the *Ylfat1::URA3ex* deletion cassette (Fig. 1 and Table 1). We then analysed the growth of the deletion mutant (JMY3148) on fatty-acid-containing medium by conducting drop tests on plates that contained either glucose or oleate as the carbon source. JMY2900, a prototrophic derivative of Po1d, was used as the control (Table 1). The two strains did not differ in their growth on YNB glucose medium, which suggests that *YlFAT1* is not an essential gene (Supporting Information, Fig. S1a). Surprisingly, Δ*Ylfat1* exhibited normal growth on oleate-based medium (Fig. S1b). As leucine auxotrophy can have genotype-dependent effects on a strain's ability to utilise hydrophobic substrates (Mauersberger *et al.*, 2001), we created strain JMY3240, a prototrophic derivative of JMY3148. No differences in growth were observed between WT and the Δ*Ylfat1* (JMY3240) strains regardless of fatty acid chain length (C6:0, C10:0, C14:0, C16:0 or C18:1; Fig. 4). This result shows that YlFat1p does not play a major role in fatty acid uptake, which suggests that at least one other protein has this function or perhaps compensates for the absence of YlFat1p in the deletion mutant. Two carrier systems have been proposed to be involved in fatty acid transport (Kohlwein & Paltauf, 1984; Papanikolaou & Aggelis, 2003; Thevenieau *et al.*, 2007); however, the genes encoding for hydrophobic substrate (alkane and fatty acid) transport remain to be identified in *Y. lipolytica*. Another explanation could be that FAs enter into the cell by diffusion or facilitated diffusion.

Deletion of *Ylfat1* improves FA accumulation in oleate-based medium

To better understand the role of YlFat1p, we analysed the effects of its presence or absence on FA accumulation. Δ*Ylfat1* and WT strains were cultivated for 24 h in $YNBD_{0.5}O_3$ medium, which favours lipid accumulation. The oleic acid used in this study contained 73% C18:1 (n-9), 7% C18:2(n-6), 4.7% C16:1(n-7), 3.9% C16:0 and 0.9% C16:1(n-9). Unexpectedly, Δ*Ylfat1* cells contained larger lipid bodies than did the WT cells, suggesting that the deletion of *YlFAT1* increases the accumulation of FAs (Fig. 5a, panel 2 compared to panel 1). Indeed, FA accumulation was 50% higher in Δ*Ylfat1* than in the WT strain: CDW attributable to FAs was 37% and 24%, respectively (Fig. 5b). In addition, the FA profiles found in the cells of the two strains were very similar, except that the Δ*Ylfat1* cells contained levels of C16:1 (4.4%) that were *c.* 2.5-fold lower than those in the WT cells (10%; Fig. 5c). This pattern was mainly due to a twofold

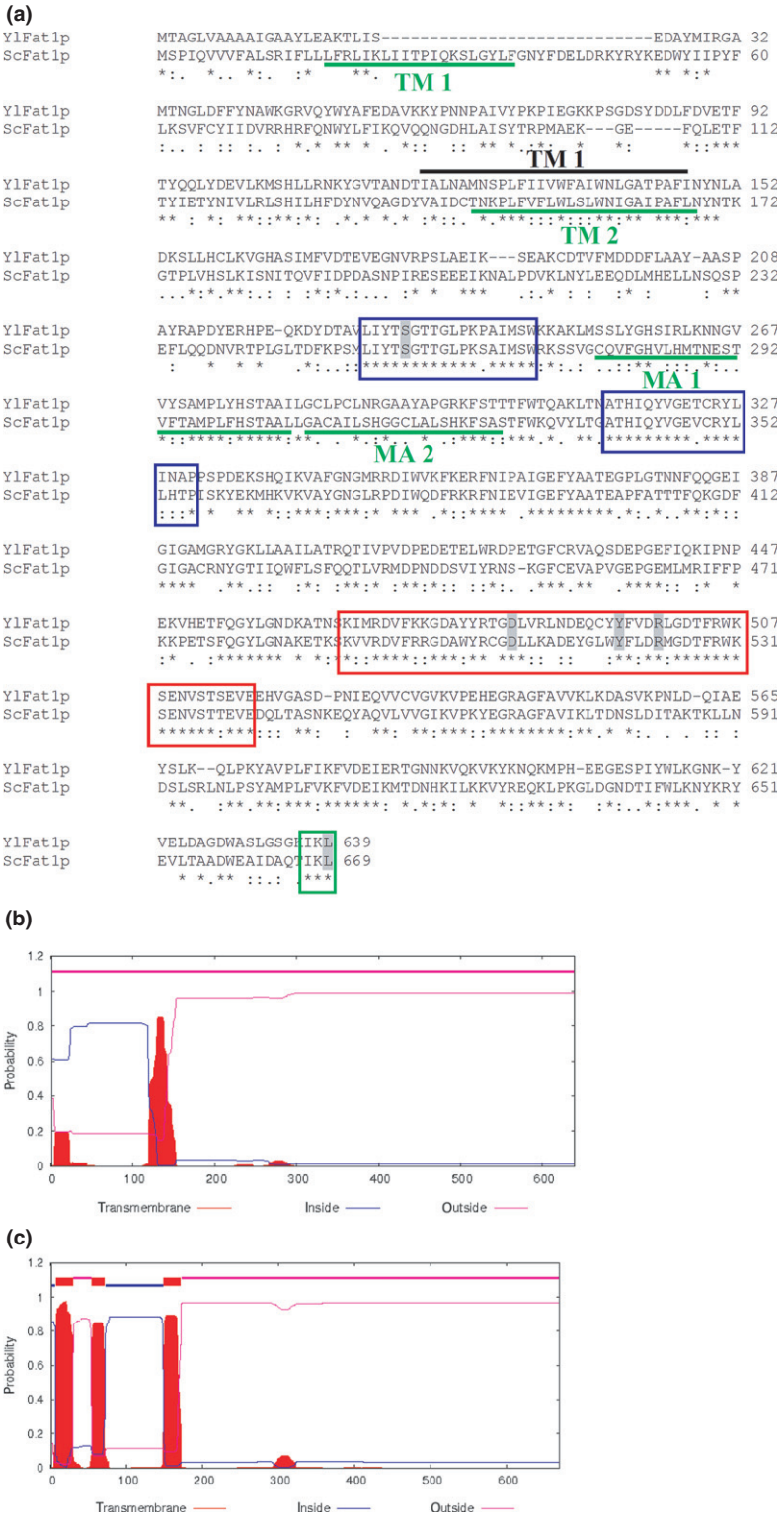

Fig. 2. Comparison of ScFat1p and YlFat1p. (a) Amino acid alignment obtained from ClustalW. The blue, red and green boxes enclose the ATP/AMP, the FATP/VLACS motifs and the PTS1 sequence, respectively. Potential YlFat1p TMs found using TMHMM ver. 2 (www.cbs.dtu.dk/services/TMHMM/) are underlined in black, while the potential TMs or membrane anchors (MAs) of ScFat1p, as per Obermeyer *et al.* (2007), are underlined in green. Amino acids in grey are essential to protein function (Zou *et al.*, 2002). (b) TMHMM profiles of YlFat1p and (c) ScFat1p.

decrease in C16:1(n-7), from 7% (± 1.77) in the WT to 3.5% (± 1.2) in Δ*Ylfat1*, and also reflected a threefold decrease in C16:1(n-9), from 3% (± 1) in the WT to only 0.9% (± 0.2) in Δ*Ylfat1*. The differing patterns obtained for these FAs can be traced back to different processes, as C16:1(n-7) accumulates in cells as a result of

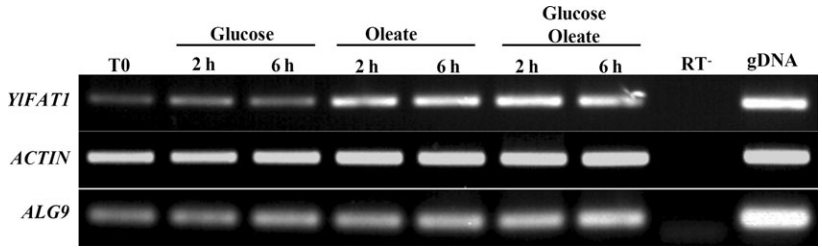

Fig. 3. Expression profile of *YlFAT1* in the presence of glucose and oleate. Precultures were grown for 15 h at 28 °C (T0) in liquid YNB supplemented with 1% glucose and 0.5% yeast extract; they were then transferred to fresh liquid YNB medium supplemented with 1% glucose, 3% oleic acid or both 1% glucose and 3% oleic acid. RT-PCR was performed on cells incubated for 2 and 6 h postinoculation. *Actin* and *ALG9* were used as endogenous controls for all the conditions tested. RT-DNA and gDNA were the RT- and gDNA controls, respectively.

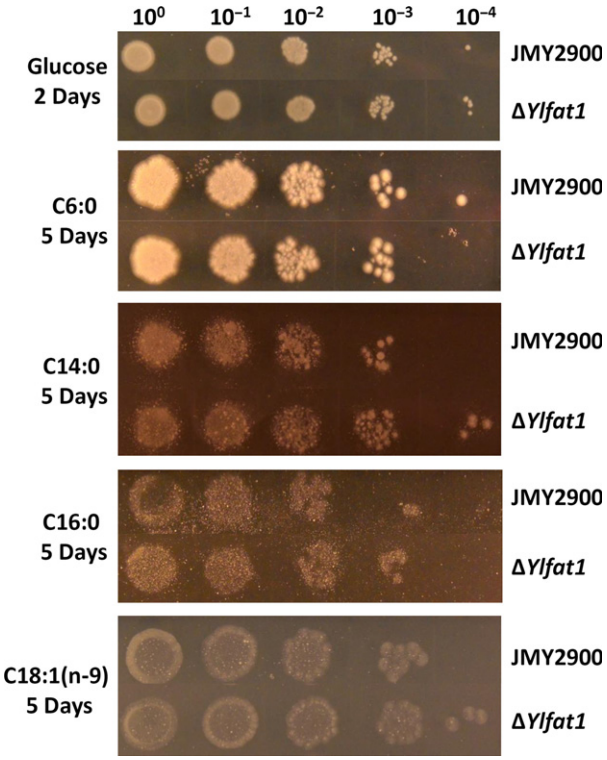

Fig. 4. Growth of the WT (JMY2900) and Δ*Ylfat1* (JMY3240) strains on media containing glucose or FAs of different chain lengths. The carbon sources were as follows: glucose, methyl caproate (C6:0), methyl decanoate (C10:0), methyl myristate (C14:0), methyl palmitate (C16:0) and oleic acid [C18:1(n-9)]. Pictures were taken after 2 or 5 days and depict three independent experiments.

both FA synthesis and the internalisation of external C16:1(n-7) present in the medium, whereas C16:1(n-9) accumulates in cells as a result of the first cycle of C18:1 (n-9; oleic acid) degradation by β-oxidation. Moreover, as the FA accumulation profile in *Y. lipolytica* generally reflects the FA profile of the extracellular medium (Beopoulos *et al.*, 2008), the decrease in C16:1(n-7) in Δ*Ylfat1* cells was likely due to the impaired entry of C16:1(n-7) into the cells, suggesting that YlFat1p is at least partially involved in the uptake of C16:1(n-7).

Because C18:1(n-9) is normally broken down via β-oxidation, we can interpret the increased accumulation of this fatty acid in Δ*Ylfat1* cells (78% as compared to 69% for the WT; Fig. 5c) as a sign of impaired β-oxidation. However, Δ*Ylfat1* strains grew similarly to the WT strain on oleate-based substrates, indicating that, although the efficiency of the β-oxidation of oleate may have been reduced in mutant strains, the remaining activity sufficed for normal growth. A potential explanation for the reduction in β-oxidation activity could be that oleate transport into the peroxisomes of Δ*Ylfat1* cells was less efficient than that into the WT cells. Another explanation for the increase in FA accumulation in Δ*Ylfat1* could be that the uptake of FAs was faster than in the reference strain, implying that β-oxidation is a saturable process and that the excess oleic acid is converted into triglycerides and stored in lipid bodies. Alternatively, this result may derive from the very efficient activation of FAs by acyl-CoA synthetases. Indeed, we recently identified 11 genes involved in the cytosolic and peroxisomal activation of FAs for which overexpression increased the amount of triglycerides stored in lipid bodies.

Lipid remobilisation is impaired in Δ*Ylfat1*

To further investigate the role of YlFat1p in *Y. lipolytica*'s physiology, we analysed lipid remobilisation in Δ*Ylfat1* cells. First, cells were grown for 24 h in $YNBD_{0.5}O_3$ medium, which favours lipid accumulation. They were then washed and resuspended in $YNBC_0$ medium (no carbon source) for the remobilisation test, which tracked FA and TAG remobilisation (Dulermo *et al.*, 2013). Interestingly, remobilisation activity in Δ*Ylfat1* was reduced compared to that in WT, with FA remobilisation rates of *c.* −1.1% of FA CDW h^{-1} ($R = 0.89$) and *c.* −1.6% of FA CDW h^{-1} ($R = 0.92$), respectively (Fig. 6a).

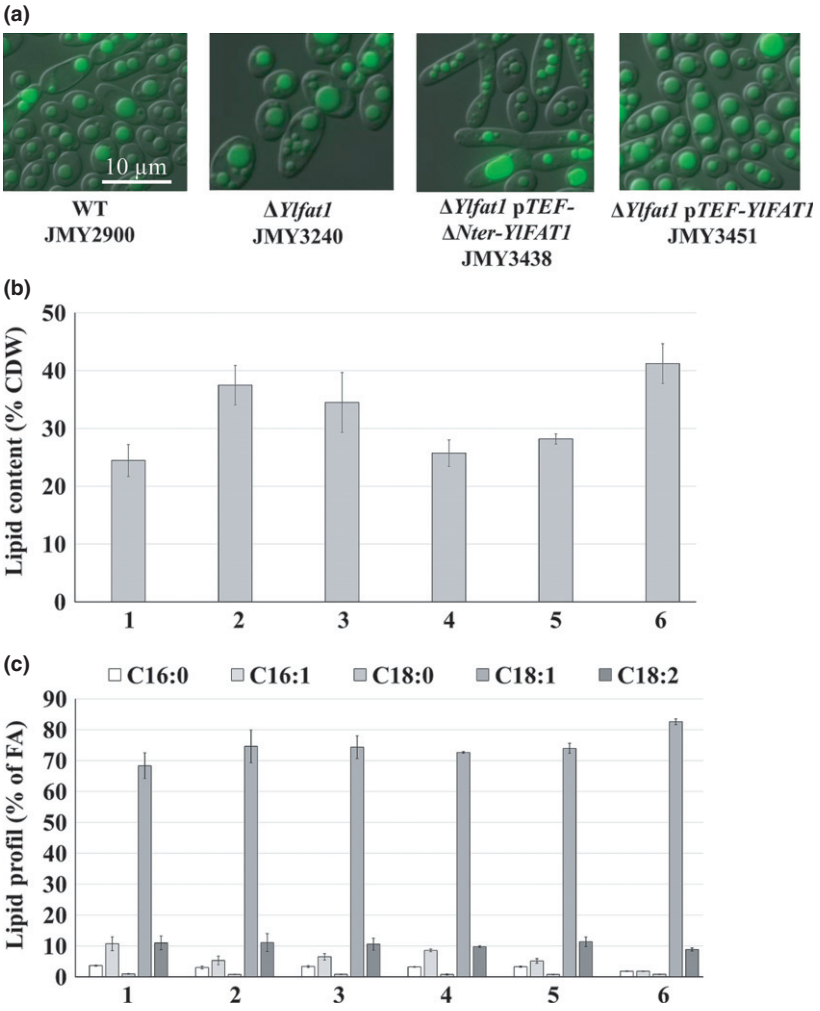

Fig. 5. Phenotype of WT (JMY2900), Δ*Ylfat1* (JMY3240), Δ*Ylfat1* p*TEF-ΔNter-YlFAT1* (JMY3438), Δ*Ylfat1* p*TEF-YlFAT1* (JMY3451), Δ*Ylfat1* p*TEF-ΔNter-YlFAT1-RedStar2* (JMY3792) and Δ*Ylfat1* p*TEF-YFP-ΔNter-YlFAT1* (JMY4170) after 24 h of culture in FA accumulation medium $YNBD_{0.5}O_3$. (a) Cell morphology after 24 h of culture in $YNBD_{0.5}O_3$. Lipid bodies were stained with BodiPy. (b) FA content in the $YNBD_{0.5}O_3$ culture was determined by GC. (c) Fatty acid profiles show the lipid fraction as a percentage of the main lipids accumulated. 1 – WT; 2 – Δ*Ylfat1*; 3 – Δ*Ylfat1* p*TEF-YlFAT1*; 4 – Δ*Ylfat1* p*TEF-ΔNter-YlFAT1*; 5 – Δ*Ylfat1* p*TEF-ΔNter-YlFAT1-RedStar2*; 6 – Δ*Ylfat1* p*TEF-YFP-ΔNter-YlFAT1*.

To determine whether *YlFAT1* overexpression restores the WT phenotype of Δ*Ylfat1* strains (i.e. restoring FA accumulation, C18:1(n-9) level, C16:1 level and remobilisation rates to WT levels), the *YlFAT1* expression cassette (p*TEF-YlFAT1*) was introduced into Δ*Ylfat1*, creating strain JMY3451. Surprisingly, neither FA accumulation nor C18:1(n-9) and C16:1 levels (Fig. 5a–c) could be restored, which suggests that the introduced YlFat1p proteins were nonfunctional (remobilisation was not tested with this strain). To investigate this hypothesis, we investigated the *Y. lipolytica* genome. During manual curation of the genome (Dujon *et al.*, 2004), the first methionine of the ORF had been defined as the start of the *YlFAT1* gene. However, we had recently performed an RNAseq sequencing analysis which had indicated that the *YlFAT1* gene is shorter: it starts at the second methionine (Fig. 1, C. Neuveglise, pers. commun.). To confirm this finding, a Δ*Nter-YlFAT1* version of the expression cassette (with the potential mitochondrial-targeting sequence deleted) was constructed and introduced into Δ*Ylfat1* (yielding strain JMY3438). Δ*Nter-YlFAT1* overexpression in Δ*Ylfat1* restored all the WT phenotypes, indicating that the second methionine corresponded to the correct start codon for *YlFAT1*. Indeed, lipid accumulation accounted for 28% of CDW, with 8.5% of FAs in the form of C16:1 (Fig. 5a panel 3, b, and c line 4). Interestingly, JMY3438 also showed a higher FA remobilisation rate than did the WT, *c.* −2.3% of FA CDW h^{-1} ($R = 0.98$; Fig. 6a), suggesting that the overexpression of Δ*Nter-YlFAT1* increased lipid remobilisation. During remobilisation, the FA profile changes observed in the complemented strain (JMY3438, Δ*fat1* Δ*Nter-YlFAT1*) were quite similar to those observed in the WT (Fig. 6b–e): overtime, the levels of C16:0 (Fig. 6b) and C16:1(n-7) decreased slightly (Fig. 6d) and the levels of C16:1(n-9; Fig. 6c) and C18:1(n-9) increased slightly (Fig. 6e). In contrast, the FA profile of the Δ*Ylfat1* strain displayed consistently low levels of C16:1(n-9; under 1% of total lipids;

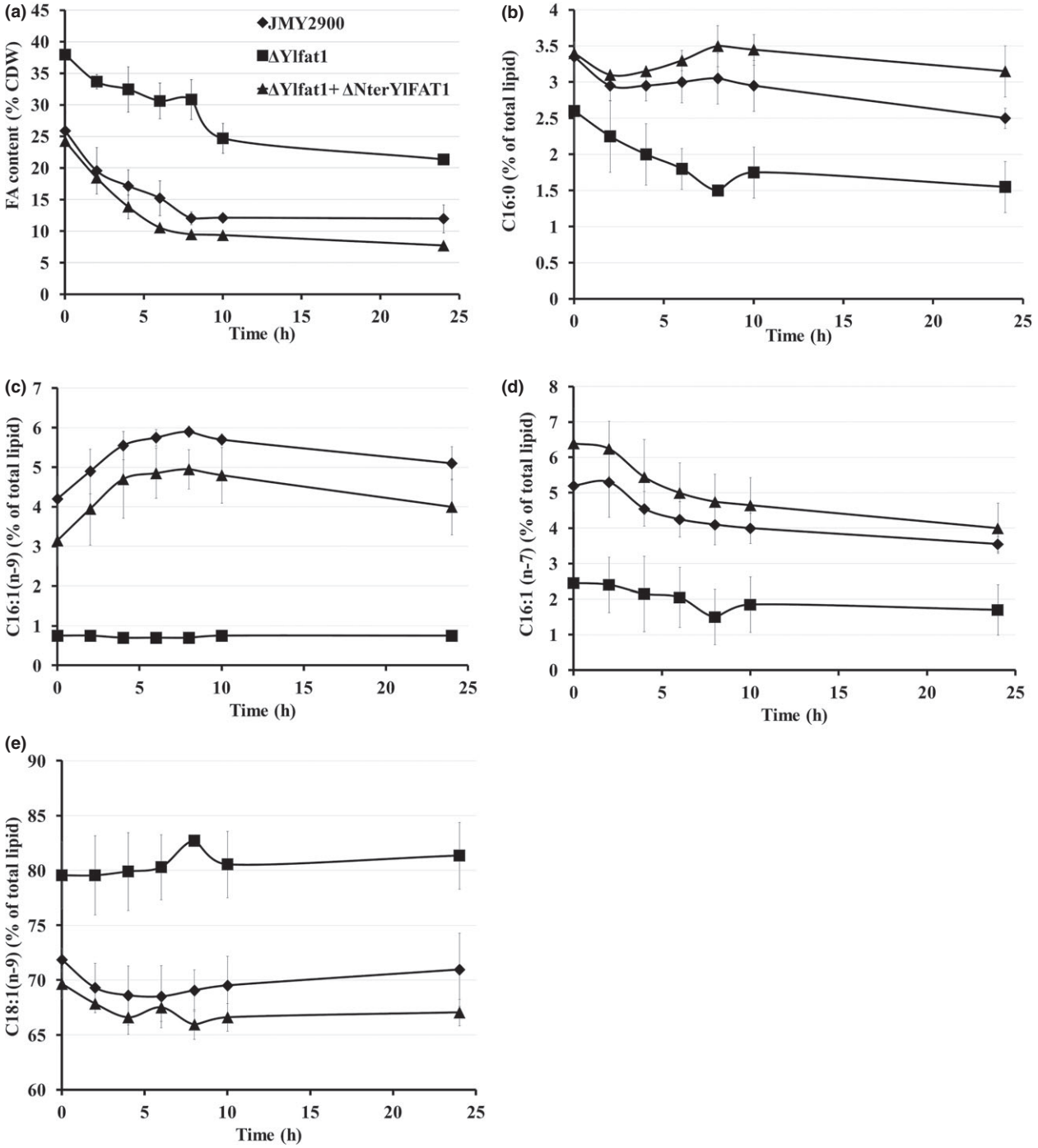

Fig. 6. Variation in FA content in WT (JMY2900), Δ*Ylfat1* (JMY3240) and Δ*Ylfat1* p*TEF*-Δ*Nter-YlFAT1* (JMY3438) during lipid remobilisation in $YNBC_0$ medium. Variation in levels of (a) total FA content, (b) C16:0, (c) C16:1(n-9), (d) C16:1(n-7) and (e) C18:1(n-9) during remobilisation.

Fig. 6c) and higher levels of C18:1(n-9; 80% vs. 70% for the WT; Fig. 6e). Surprisingly, however, C16:0 levels decreased more in Δ*Ylfat1* than in WT during the first 10 h of culture (Fig. 6b). When taken together, these results demonstrate that YlFat1p plays an important role in FA remobilisation. This result could also explain the higher C18:1(n-9) and lower C16:1(n-9) levels observed in Fig. 5 as C18:1(n-9) is sequestered in lipid bodies.

YlFat1p localisation

In *S. cerevisiae*, ScFat1p is localised to plasma membranes (PMs), peroxisomes, lipid bodies and the endoplasmic reticulum. Localisation to these different addresses in the cell involves both the TM at the N-terminus and the peroxisome-targeting sequence at the C-terminus (Choi & Martin, 1999; van Roermund *et al.*, 2012; Kohlwein *et al.*, 2013).

To determine YlFat1p localisation patterns in *Y. lipolytica*, fusion proteins were constructed at both the C-terminus and the N-terminus as previously performed in *S. cerevisiae* by Choi & Martin (1999). First, the red fluorescent protein (RedStar2p) was fused to the C-terminus of Δ*NterYlFAT1* (creating Δ*Nter-YlFAT1-Redstar2*). Second, the yellow fluorescent protein (YFP) was fused to the N-terminus of Δ*NterYlFAT1* (*YFP-ΔNter-YlFAT1*). These protein fusions were then expressed under the p*TEF* promoter (Müller *et al.*, 1998) in strain JMY3148 (Δ*Ylfat1*), yielding strains JMY3792 and JMY4170, respectively. Whereas overexpression of YFP-ΔNter-YlFAT1p did not restore lipid content and C16:1 levels to WT values (Fig. 5b and c, number 6), overexpression of Δ*Nter-YlFAT1-Redstar2* restored the lipid accumulation phenotype (Fig. 5b, number 5) but not C16:1 levels (which were still only 5% of total lipid content; Fig. 5c, number 5). These results suggest that ΔNter-YlFat1-RedStar2p was partially functional. Using the microscope, we observed that YFP-ΔNter-YlFat1p was localised in the peroxisomes (Fig. 7a), whereas ΔNter-YlFat1-RedStar2p was localised at the surface of the lipid bodies (more precisely, it seems to be at the interface between closed lipid bodies; Fig. 7b). The absence of fluorescence in the PMs might have resulted from either (1) levels of the protein that were too low to be detected or (2) an absence of the protein in the PMs. The absence of the fluorescent protein in the PMs might have been due to fusions between RedStar2 and YFP or to the fact that YlFat1p does not have the first TM that is found in ScFat1p. Interestingly, the observation that YlFat1p localises between lipid bodies is similar to an observation that was made in a previous study of Tgl4-YFPp localisation (Dulermo *et al.*, 2013). Tgl4p is an intracellular lipase involved in TAG degradation (Dulermo *et al.*, 2013), and it is possible that Tgl4p and YlFat1p

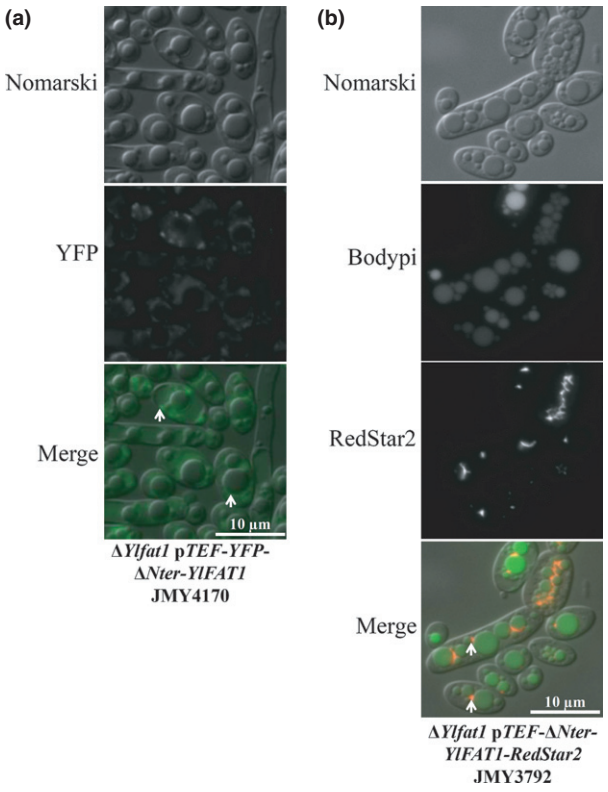

Fig. 7. Localisation of ΔNter-YlFat1-RedStar2p and YFP-ΔNter-YlFat1p. Localisation of (a) YFP-ΔNter-YlFat1p and (b) ΔNter-YlFat1-RedStar2p after 24 h of culture in $YNBD_{0.5}O_3$ medium. In (b), lipid bodies were stained with BodiPy.

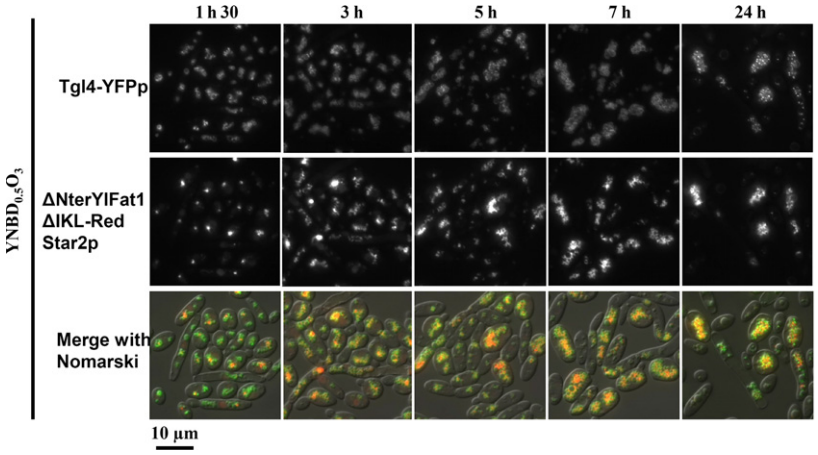

Fig. 8. Localisation of ΔNterYlFAT1-RedStar2p and Tgl4-YFP during 24 h of culture in $YNBD_{0.5}O_3$ medium. Fluorescence was observed for 24 h.

coexist, either in close proximity to each other or joined together in a protein complex. To determine whether *Yl-FAT1* and Tgl4-YFPp colocalise, p*TEF-TGL4-YFP* was introduced into JMY3792, which expressed Δ*Nter-YlFAT1-RedStar2* (generating JMY3919). Cells were cultivated in $YNBD_{0.5}O_3$, and fluorescence was monitored for 24 h. We observed that ΔNter-YlFat1-RedStar2p and Tgl4-YFPp only rarely colocalised (Fig. 8), suggesting that they do not form a complex. However, our observations suggest that lipid bodies have regions where at least some proteins were present when yeast were grown in $YNBD_{0.5}O_3$.

Conclusions

The aim of this study was to explore the role of Fat1p in the oleaginous yeast *Y. lipolytica*. In *S. cerevisiae*, ScFat1p has been described as an LCFA transporter which is necessary for growth on FA-based substrates and which is localised in the plasma membrane, endoplasmic reticulum, peroxisomes and lipid bodies. However, our study reveals that YlFat1p in *Y. lipolytica* has evolved differently: it plays a dissimilar role and demonstrates a different localisation pattern. Indeed, after redefining its ORF, we found that *YlFAT1* is induced by oleic acid and is not required for growth on FA-containing media; these results do not match those found for *ScFAT1*. Moreover, the Δ*Ylfat1* strains differed from the WT strain in many phenotypic traits: they had a higher FA content (37% vs. 24%) and a modified FA profile, where C18:1(n-9) content was higher (78% vs. 69%) and C16:1 content was lower (twofold and threefold lower levels of C16:1(n-7) and C16:1(n-9), respectively). Taken together, these results demonstrate that YlFat1p is necessary for the optimal oxidation of C18:1(n-9). Additionally, YlFat1p also differs from ScFat1p in that it displays a much more restricted localisation pattern. The differences in function and localisation between YlFat1p and ScFat1p described here may stem from structural differences between the two proteins (one TM vs. two TMs and two membrane anchors, respectively). The lack of functionality observed for YFP-ΔNter-YlFAT1p prevents us from arriving at any conclusions regarding the potential peroxisomal localisation of YlFat1, although we do not exclude this possibility. However, when taken together, the various results of this study suggest that YlFat1p may export FAs from lipid bodies, thus favouring their breakdown during remobilisation. A recent review by R Fukuda (2013) of n-alkane metabolism in *Y. lipolytica* discusses the role of YlFat1p in alkane metabolism. YlFat1p was reported to be essential for growth on n-decane and n-dodecane and necessary for growth on n-tetradecane and n-hexadecane. Combined with our results, this finding suggests that YlFat1p could also be involved in the activation of short-chain FAs and their transport from the cytosol into the peroxisome during growth on alkanes. These results regarding the role of Fat1p represent the first step in the analysis of lipid homeostasis in the oleaginous yeast *Yarrowia lipolytica* and demonstrate that, although *S. cerevisiae* and *Y. lipolytica* are similar in many aspects of fatty acid metabolism, they are not identical. In *Y. lipolytica*, lipid homeostasis relies on equilibrium among multiple pathways, involving at least two distinct transport systems that remain to be identified, and probably also diffusion or facilitated diffusion. In addition, lipid homeostasis in *Y. lipolytica* involves an efficient cytosolic and peroxisomal fatty acid activation pathway that requires eleven genes (R. Dulermo, H. Gamboa-Meléndez, J. M. Nicaud, unpublished), as well as the subsequent routing of the activated FAs into either the storage pathway, in which they are stored as triglycerides, or the β-oxidation pathway, in which they are broken down. Additionally, the presence of the fatty-acid-binding protein (FABP), identified in *Y. lipolytica* by Dell'Angelica *et al.* (1992), may result in buffering between free FAs and activated derivative acyl-CoA.

Acknowledgements

This work was supported by FIDOP/FASO funds (fonds d'action stratégique des oléagineux) from the French vegetable oil and protein production industry. We also thank F. Brunel for JMY2900 strain. We would also like to thank Jessica Pearce and Lindsay Higgins for their language editing services.

References

Barth G & Gaillardin C (1996) *Yarrowia lipolytica. Non conventional yeasts in biotechnology, a handbook* (Wolf K Ed), pp. 313–388. Springer, Berlin.

Beopoulos A, Mrozova Z, Thevenieau F, Le Dall MT, Hapala I, Papanikolaou S, Chardot T & Nicaud JM (2008) Control of lipid accumulation in the yeast *Yarrowia lipolytica*. *Appl Environ Microbiol* **74**: 7779–7789.

Beopoulos A, Cescut J, Haddouche R, Uribelarrea JL, Molina-Jouve C & Nicaud JM (2009) *Yarrowia lipolytica* as a model for bio-oil production. *Prog Lipid Res* **48**: 375–387.

Beopoulos A, Nicaud JM & Gaillardin C (2011) An overview of lipid metabolism in yeasts and its impact on biotechnological processes. *Appl Microbiol Biotechnol* **90**: 1193–1206.

Browse J, McCourt PJ & Somerville CR (1986) Fatty acid composition of leaf lipids determined after combined digestion and fatty acid methyl ester formation from fresh tissue. *Anal Biochem* **152**: 141–145.

Choi JY & Martin CE (1999) The *Saccharomyces cerevisiae FAT1* gene encodes an acyl-CoA synthetase that is required

for maintenance of very long chain fatty acid levels. *J Biol Chem* **274**: 4671–4683.

Claros MG & Vincens P (1996) Computational method to predict mitochondrially imported proteins and their targeting sequences. *Eur J Biochem* **241**: 779–786.

Dell'Angelica EC, Stella CA, Ermacora MR, Ramos EH & Santome JA (1992) Study on fatty acid binding by proteins in yeast. Dissimilar results in *Saccharomyces cerevisiae* and *Yarrowia lipolytica*. *Comp Biochem Physiol B* **102**: 261–265.

Dirusso CC, Connell EJ, Faergeman NJ, Knudsen J, Hansen JK & Black PN (2000) Murine *FATP* alleviates growth and biochemical deficiencies of yeast *fat1*Delta strains. *Eur J Biochem* **267**: 4422–4433.

Dujon B, Sherman D, Fischer G *et al.* (2004) Genome evolution in yeasts. *Nature* **430**: 35–44.

Dulermo T, Tréton B, Beopoulos A, Kabran Gnankon AP, Haddouche R & Nicaud JM (2013) Characterization of the two intracellular lipases of *Y. lipolytica* encoded by *TGL3* and *TGL4* genes: new insights into the role of intracellular lipases and lipid body organisation. *Biochim Biophys Acta* **1831**: 1486–1495.

Duronio RJ, Knoll LJ & Gordon JI (1992) Isolation of a *Saccharomyces cerevisiae* long chain fatty acyl: CoA synthetase gene (*FAA1*) and assessment of its role in protein N-myristoylation. *J Cell Biol* **117**: 515–529.

Faergeman NJ, DiRusso CC, Elberger A, Knudsen J & Black PN (1997) Disruption of the *Saccharomyces cerevisiae* homologue to the murine fatty acid transport protein impairs uptake and growth on long-chain fatty acids. *J Biol Chem* **272**: 8531–8538.

Fickers P, Le Dall MT, Gaillardin C, Thonart P & Nicaud JM (2003) New disruption cassettes for rapid gene disruption and marker rescue in the yeast *Yarrowia lipolytica*. *J Microbiol Methods* **55**: 727–737.

Fukuda R (2013) Metabolism of hydrophobic carbon sources and regulation of it in n-alkane-assimilating yeast *Yarrowia lipolytica*. *Biosci Biotechnol Biochem* **77**: 1149–1154.

Haddouche R, Delessert S, Sabirova J, Neuvéglise C, Poirier Y & Nicaud JM (2010) Roles of multiple acyl-CoA oxidases in the routing of carbon flow towards β-oxidation and polyhydroxyalkanoate biosynthesis in *Yarrowia lipolytica*. *FEMS Yeast Res* **10**: 917–927.

Johnson DR, Knoll LJ, Levin DE & Gordon JI (1994) *Saccharomyces cerevisiae* contains four fatty acid activation (*FAA*) genes: an assessment of their role in regulating protein N-myristoylation and cellular lipid metabolism. *J Cell Biol* **127**: 751–762.

Kabran P, Rossignol T, Gaillardin C, Nicaud JM & Neuvéglise C (2012) Alternative splicing regulates targeting of malate dehydrogenase in *Yarrowia lipolytica*. *DNA Res* **19**: 231–244.

Knoll LJ, Johnson DR & Gordon JI (1994) Biochemical studies of three *Saccharomyces cerevisiae* acyl-CoA synthetases, Faa1p, Faa2p, and Faa3p. *J Biol Chem* **269**: 16348–16356.

Kohlwein S & Paltauf F (1984) Uptake of fatty acids by the yeasts, *Saccharomyces uvarum* and *Saccharomycopsis lipolytica*. *Biochim Biophys Acta* **792**: 310–317.

Kohlwein SD, Veenhuis M & van der Klei IJ (2013) Lipid droplets and peroxisomes: key players in cellular lipid homeostasis or a matter of fat–store 'em up or burn 'em down. *Genetics* **193**: 1–50.

Le Dall MT, Nicaud JM & Gaillardin C (1994) Multiple-copy integration in the yeast *Yarrowia lipolytica*. *Curr Genet* **26**: 38–44.

Mauersberger S, Wang HJ, Gaillardin C, Barth G & Nicaud JM (2001) Insertional mutagenesis in the n-alkane-assimilating yeast *Yarrowia lipolytica*: generation of tagged mutations in genes involved in hydrophobic substrate utilization. *J Bacteriol* **183**: 5102–5109.

Mlícková K, Roux E, Athenstaedt K, d'Andrea S, Daum G, Chardot T & Nicaud JM (2004) Lipid accumulation, lipid body formation, and acyl coenzyme A oxidases of the yeast *Yarrowia lipolytica*. *Appl Environ Microbiol* **70**: 3918–3924.

Müller S, Sandal T, Kamp-Hansen P & Dalbøge H (1998) Comparison of expression systems in the yeasts *Saccharomyces cerevisiae*, *Hansenula polymorpha*, *Klyveromyces lactis*, *Schizosaccharomyces pombe* and *Yarrowia lipolytica*. Cloning of two novel promoters from *Yarrowia lipolytica*. *Yeast* **14**: 1267–1283.

Natter K, Leitner P, Faschinger A, Wolinski H, McCraith S, Fields S & Kohlwein SD (2005) The spatial organization of lipid synthesis in the yeast *Saccharomyces cerevisiae* derived from large scale green fluorescent protein tagging and high resolution microscopy. *Mol Cell Proteomics* **4**: 662–672.

Nicaud JM, Madzak C, van den Broek P, Gysler C, Duboc P, Niederberger P & Gaillardin C (2002) Protein expression and secretion in the yeast *Yarrowia lipolytica*. *FEMS Yeast Res* **2**: 371–379.

Obermeyer T, Fraisl P, DiRusso CC & Black PN (2007) Topology of the yeast fatty acid transport protein Fat1p: mechanistic implications for functional domains on the cytosolic surface of the plasma membrane. *J Lipid Res* **48**: 2354–2364.

Papanikolaou S & Aggelis G (2003) Modeling lipid accumulation and degradation in *Yarrowia lipolytica* cultivated on industrial fats. *Curr Microbiol* **46**: 398–402.

Querol A, Barrio E, Huerta T & Ramón D (1992) Molecular monitoring of wine fermentations conducted by active dry yeast strains. *Appl Environ Microbiol* **58**: 2948–2953.

Sambrook J, Maniatis T & Fritsch EF (1989) *Molecular Cloning: A Laboratory Manual*, 2nd edn. Cold Spring Harbor Laboratory, Cold Spring Harbor.

Thevenieau F, Le Dall MT, Nthangeni B, Mauersberger S, Marchal R & Nicaud JM (2007) Characterization of *Yarrowia lipolytica* mutants affected in hydrophobic substrate utilization. *Fungal Genet Biol* **44**: 531–542.

van Roermund CW, Ijlst L, Majczak W, Waterham HR, Folkerts H, Wanders RJ & Hellingwerf KJ (2012)

Peroxisomal fatty acid uptake mechanism in *Saccharomyces cerevisiae*. *J Biol Chem* **287**: 20144–20153.

Watkins PA, Lu JF, Steinberg SJ, Gould SJ, Smith KD & Braiterman LT (1998) Disruption of the *Saccharomyces cerevisiae FAT1* gene decreases very long-chain fatty acyl-CoA synthetase activity and elevates intracellular very long-chain fatty acid concentrations. *J Biol Chem* **273**: 18210–18219.

Zou Z, DiRusso CC, Ctrnacta V & Black PN (2002) Fatty acid transport in *Saccharomyces cerevisiae*. Directed mutagenesis of *FAT1* distinguishes the biochemical activities associated with Fat1p. *J Biol Chem* **277**: 31062–31071.

Zou Z, Tong F, Faergeman NJ, Børsting C, Black PN & DiRusso CC (2003) Vectorial acylation in *Saccharomyces cerevisiae*. Fat1p and fatty acyl-CoA synthetase are interacting components of a fatty acid import complex. *J Biol Chem* **278**: 16414–16422.

Supporting Information

Additional Supporting Information may be found in the online version of this article:

Fig. S1. Growth of wild-type (JMY2900) and Δ*Ylfat1* (JMY3240) strains in (a) microplates containing $YNBD_{0.1}$ liquid medium with glucose 0.1% and in (b) Erlenmeyer flasks containing liquid $YNBO_{0.1}Y_{0.05}$ medium with oleic acid 0.1% supplemented with 0.05% yeast extract.